Mechanical interaction between historical brick and repair mortar: experimental and numerical tests

2011 J. Phys.: Conf. Ser. 305 012126

(http://iopscience.iop.org/1742-6596/305/1/012126)

Journal of Physics: Conference Series **305** (2011) 012126 doi:10.1088/1742-6596/305/1/012126

Mechanical interaction between historical brick and repair mortar: experimental and numerical tests

P Bocca, A Grazzini, D Masera, A Alberto, S Valente

Department of Structural and Geotechnical Engineering, Politecnico di Torino, Corso Duca degli Abruzzi 24, 10129 Torino, Italy

E-mail: silvio.valente@polito.it

Abstract. An innovative laboratory procedure, developed at the Non Destructive Testing Laboratory of the Politecnico di Torino, as a preliminary design stage for the pre-qualification of repair mortars applied to historical masonry buildings is described. Tested repair mortars are suitable for new dehumidified plaster in order to stop the rising damp effects by capillary action on historical masonry walls. Long-term plaster delamination occurs frequently as a consequence of not compatible mechanical characteristics of mortar. Preventing this phenomenon is the main way to increase the durability of repair work. In this direction, it is useful to analyse, through the cohesive crack model, the evolutionary phenomenon of plaster delamination. The parameters used in the numerical simulation of experimental tests are able to characterize the mechanical behaviour of the interface. It is therefore possible to predict delamination in problems with different boundary conditions.

1. Introduction

An innovative laboratory procedure, developed at the Non Destructive Testing Laboratory of the Politecnico di Torino, as a preliminary design stage for the pre-qualification of repair mortars applied to historical masonry buildings is described. The tested repair mortars are suitable for the new dehumidified plaster in order to stop the rising damp effects by capillary action on historical masonry walls. The procedure consists in the application of static loads to mixed brick-mortar specimens having peculiar characteristics in terms of geometry and adhesion at the interface, with continuous monitoring of the longitudinal and transverse displacements. A numerical simulation based on the cohesive crack model was used to follow the experimental data, so as to describe the evolutionary phenomenon of de-bonding as a function of a small number of parameters.

2. Specimen preparation

The geometry of the specimens is shown in figure 1.

The layers of dehumidifying mortar were not applied in complete adherence to the brick support; on the contrary they were applied in symmetrical and regular discontinuity, created in the casting phase through the interposition of a thin steel leaf shown in figure 3. These discontinuities behave as notches which are able to trigger multiple crack propagation. The pre-blended mortar, chosen among the principal ones on the market, is a transpirant base render made from natural hydraulic lime and Eco-Pozzolan, suitable for the restoration of old

historical masonry damaged by rising capillary damp and sulphate salts. The Young's modulus, evaluated according to UNI6556, was 4379 MPa. The compressive strength, evaluated according to UNI6556, was 33.8 MPa. The above mentioned values were evaluated 28 days after the cast. The mixed pieces were instrumented with seven inductive miniature displacement transducers shown in figures 2 and 4. One transducer (SP0) was arranged horizontally in the low part of the specimen and connected among the two opposite mortar layers, in order to measure the displacements due to bulging. The other transducers (SP1-2-3-4 on the right, SP5-6 on the left) have been placed vertically and in sequence among them, connected between the mortar and the brick in order to record the delamination between the two materials.

3. Experimental setup

The static compressive tests were performed with the aid of a 250 kN servo controlled machine, model 810 MTS. The force transducer was based on a full extensometric bridge, linearized in the range from 0 to 25 kN. The load was applied to the specimen through a spherical hinge. A pre-determined upward velocity of 0.001 mm/s was applied to the lower machine plate (see figure 4) through a servo controlled hydraulic actuator. The specimens were subjected to static

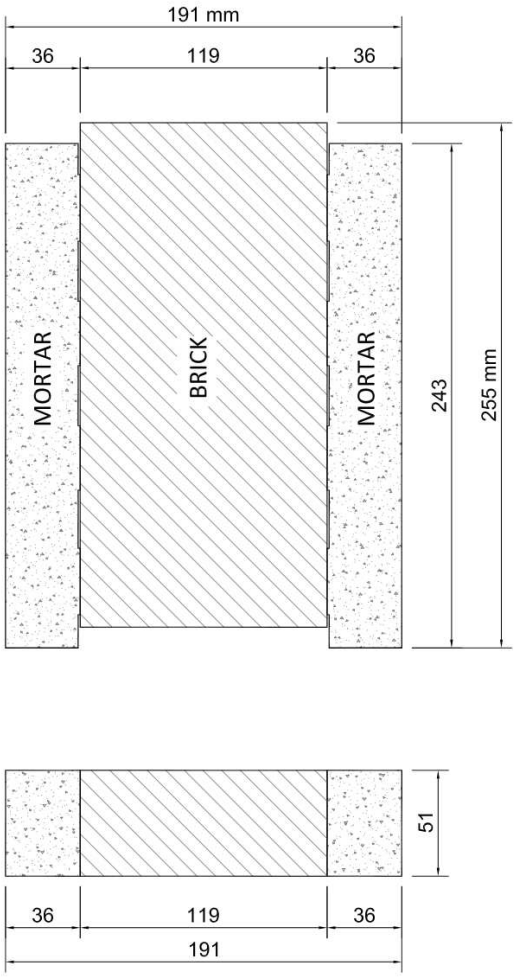

Figure 1. Geometry of specimen.

tests after 28 days of maturation. Two Teflon leaves, having thickness=1.mm, were located below the specimen in order to reduce the friction related to the horizontal expansion of the plaster. The experimental setup is shown in figure 4.

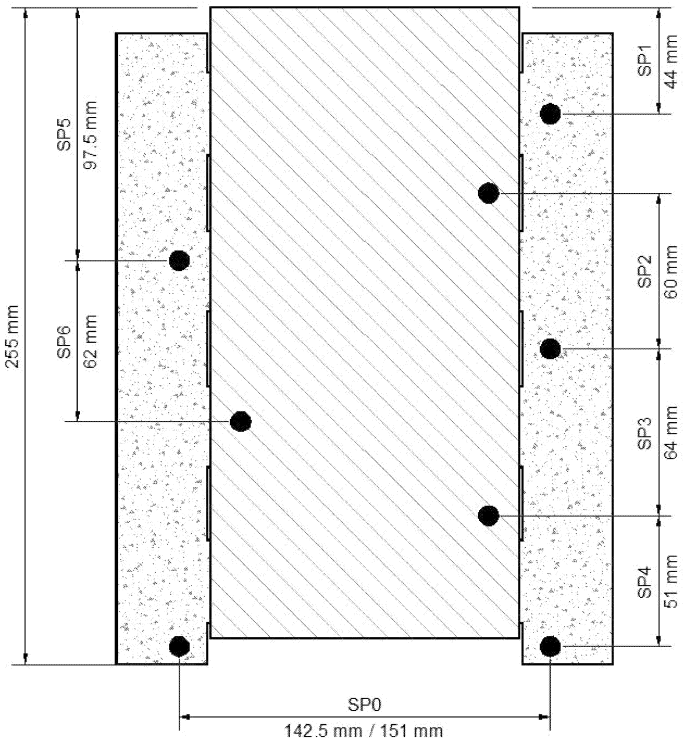

Figure 2. Transducer positions

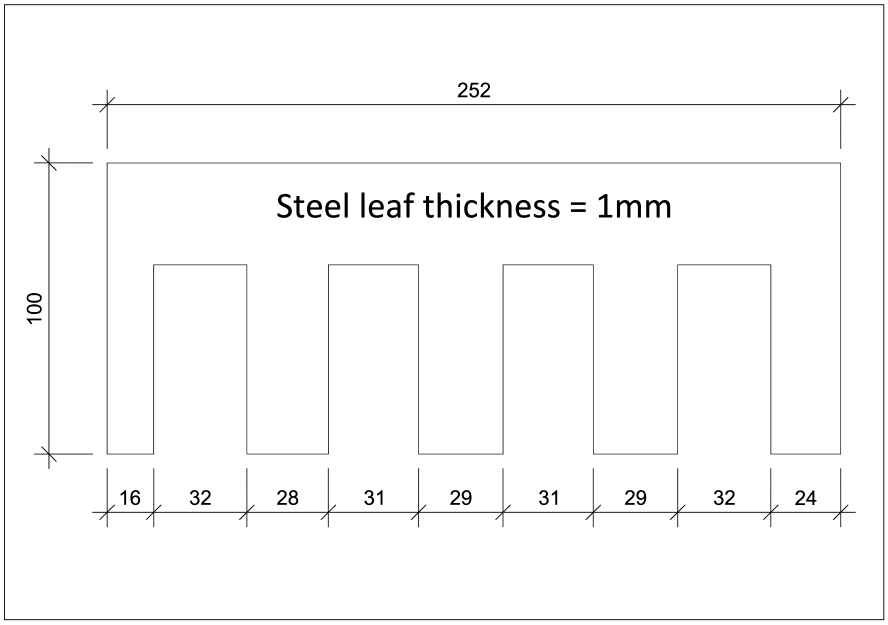

Figure 3. Steel leaf extracted after mortar solidification

4. Numerical simulation through the cohesive crack model

The most realistic method used today for the numerical simulation of mortar and brick fracture is the cohesive crack model, introduced by Barenblatt [1] and Dugdale [2] for elasto-plastic materials and by Hillerborg *et al* [3] for quasi-brittle materials. This model was applied by means of the commercially distributed code Abaqus [4], based on the Finite Element Method. In the present work the crack initiation criterion was assumed as:

$$\left(\frac{\sigma_0}{f_t}\right)^2 + \left(\frac{\tau_0}{f_s}\right)^2 = 1 \tag{1}$$

where σ_0 and τ_0 are stresses evaluated along the directions normal and tangential to the interface and f_t and f_s are the related strength assumed respectively equal 3 MPa and 4.5 MPa. The point where equation (1) is satisfied is called *fictitious crack tip*.

According to this method the cohesive stresses acting on the non-linear fracture process zone (shortened FPZ) are decreasing functions of the effective value of the displacement discontinuity [5],[6],[7], which was assumed as:

$$w_{eff} = \sqrt{\left(\frac{w_n}{w_{nc}}\right)^2 + \left(\frac{w_t}{w_{tc}}\right)^2} \tag{2}$$

Where w_n is the mutual displacement component normal to the interface and w_t the tangential one. w_{nc} and w_{tc} are the corresponding critical values assumed equal to 0.003 mm.

If $w_{eff} > 1$ no stress transfer occurs and therefore the crack is stress free. Otherwise the stresses are decreasing functions of w_{eff} following a pre-defined softening law. In the present work the above mentioned law is linear, starting from σ_0 and τ_0 and ending in the point where $w_{eff} = 1$ called *real crack tip*. The behaviour of the material outside the FPZ is linear elastic (see table 1).

From a theoretical point of view (see [8],[9]) it is expected that the peak-load of an unsymmetrical model is lower that the corresponding value related to a symmetrical model.

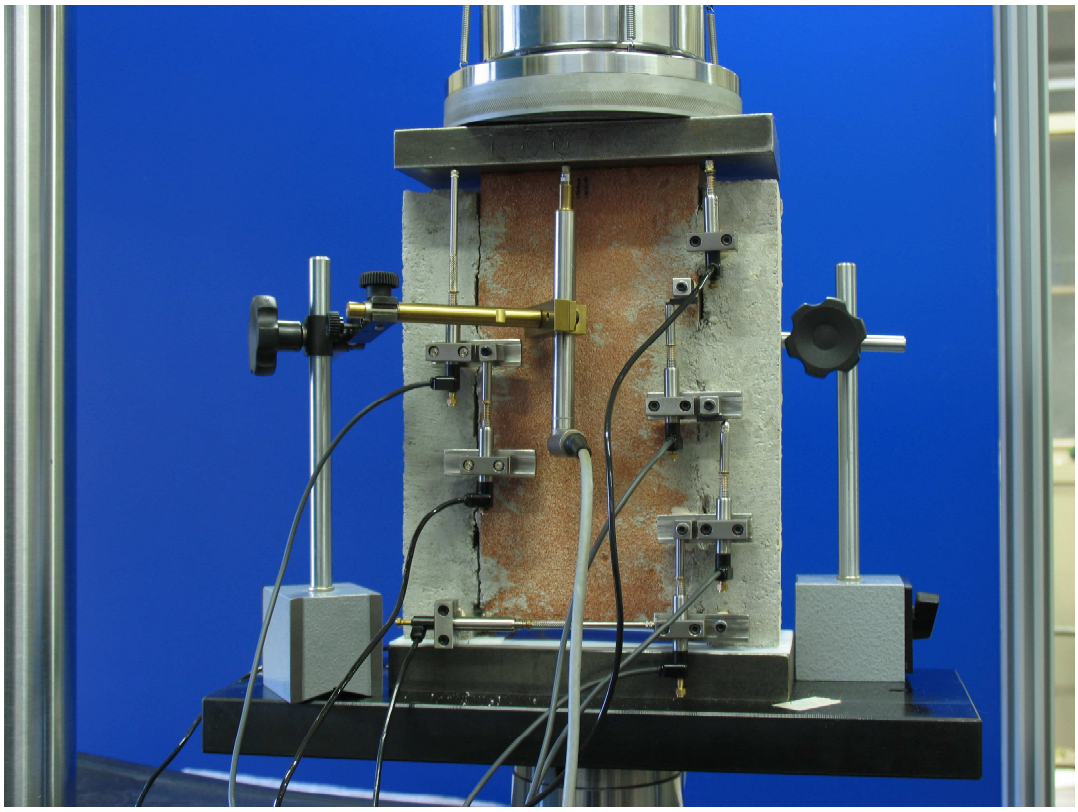

Figure 4. Experimental setup

Table 1. Elastic properties

	Young's mod MPa	Poisson -
mortar	4400	0.15
brick	8000	0.20

Table 2. Experimental and numerical results

	Max load N	Max horiz.displ. mm	Max vert.displ. mm
Specimen-1	8656	1.67	0.48
Specimen-2	5809	1.14	0.44
Simulation	6339	0.39	0.05

In order to reduce the computational work, the above mentioned theoretical observation was ignored, and a symmetrical model was analysed. The error induced by this assumption is small if compared to the scatter in the experimental results. The numerical analysis were executed by applying a pre-defined downward velocity to the upper face of the brick. Three examples of deformed finite element mesh are shown in figure 5.

5. Experimental and numerical results

The mechanical model applied does not include any time scale, neither of viscous type, nor of inertial type. Therefore it is a time-independent model. In figures 6, 7 and 8 the ordinates are divided by the maximum values shown in table 2. Experimental and numerical values of maximum load are in good agreement. Of course in the neighbourhood of the couple (f_s,f_t) assumed, other couples exist which give the same value of peak load, but a sensitivity analysis of this model is beyond the scope of the present work. After the maximum load was achieved, during the non-linear softening phase, the Newton-Raphson procedure was stopped as soon as the uniqueness of the incremental solution was lost. Therefore only an initial part of the softening phase can be simulated numerically. This is the reason why the maximum value of horizontal and vertical displacement achieved numerically was smaller than the analogous value achieved experimentally. Furthermore it is worthwhile noting that the experimental value of vertical displacement includes the contribution of Teflon leaves, which was not included in the analogous numerical value.

In figures 6, 7 and 8 a ($\triangle$) indicates the global vertical displacement. A symbol is drawn every 100 points measured or computed. Since the initial model behaviour is elastic, the mechanical response is linear and the time increment can be large. This is the reason why, independently on the time scale used, all response diagrams in figure 8 are initially linear without any symbol. In the experimental laboratory, the loading point displacements was measured as the mean value of two transducers, one on each side of the specimen (see figure 4). From an experimental point of view the initial phase is characterized by local support settlements. This is the reason of the initial irregular response diagram shown in figures 6 and 7, with many symbols drawn.

In figures 6, 7 and 8 a (□) indicates the global horizontal displacement evaluated from the mortar on the left side to the mortar on the right. In all cases this diagram shows a knee point: on the left side there are small values due to elastic deformation, on the right side large values due to the non-linear fracture process. The above mentioned knee point occurs at the time of peak-load. It means that the crack growing from the bottom to the top of the interface causes the global softening branch. This behaviour is predicted theoretically (figure 8) and confirmed experimentally (figures 6 and 7). Signals of transducers SP1 and SP5 show how experimental results break the symmetry exactly at peak load for both specimens. In case of specimen-1 the weaker interface was on the left side, as shown in figure 9. In case of specimen-2 the weaker interface was on the right side, as shown in figure 10.

6. Conclusions

- The evolutionary phenomena involved in the plaster delamination were accurately analysed by means of the experimental setup proposed.
- Through the cohesive crack model it was possible to interpret theoretically the above mentioned phenomena occurring at the interface between brick and mortar.
- As a first approximation, the set of mechanical properties used to describe the cohesive law can be used for the analysis of a problem with different boundary conditions.

7. References

[1] Barenblatt G I 1959 The formation of equilibrium cracks during brittle fracture: general ideas and hypotheses *Journal of Applied Mathematics and Mechanics*, 622-636,
[2] Dugdale D S 1960 Yielding of steel sheets containing slits. *Journal of Mechanics and Physics of Solids* **8** 100-114
[3] Hillerborg A, Modeer M and Petersson P E 1976 Analysis of crack formation and crack growth in concrete by means of fracture mechanics and finite elements *Cement and Concrete Research* **6** 773-782

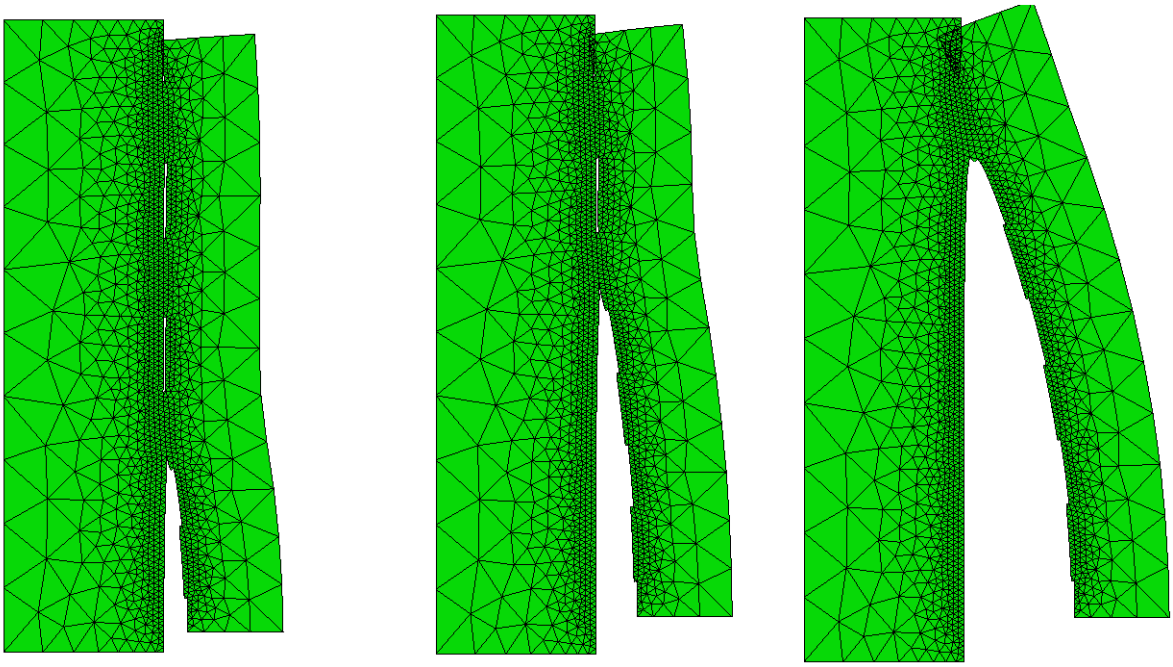

Figure 5. Finite element mesh of half specimen for step 74,135 and 151. Displacements are enlarged 500 times.

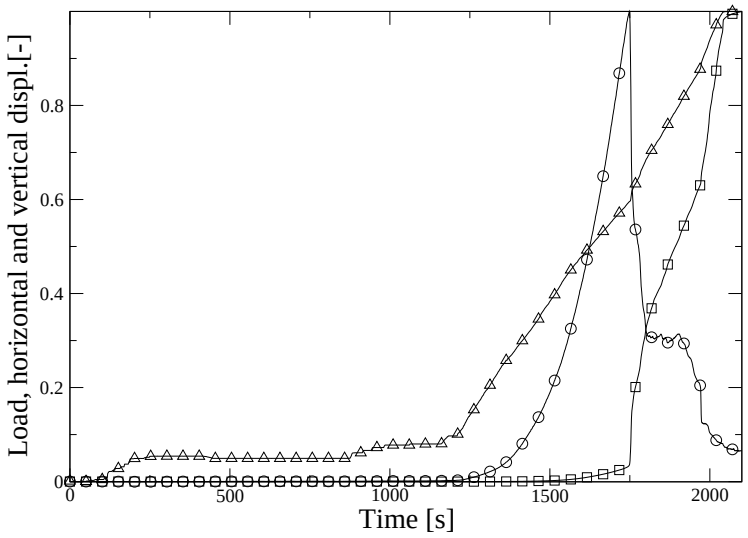

Figure 6. Experimental dimensionless results for the first specimen: (○)load, (□)horiz.displ., (△)vert.displ.

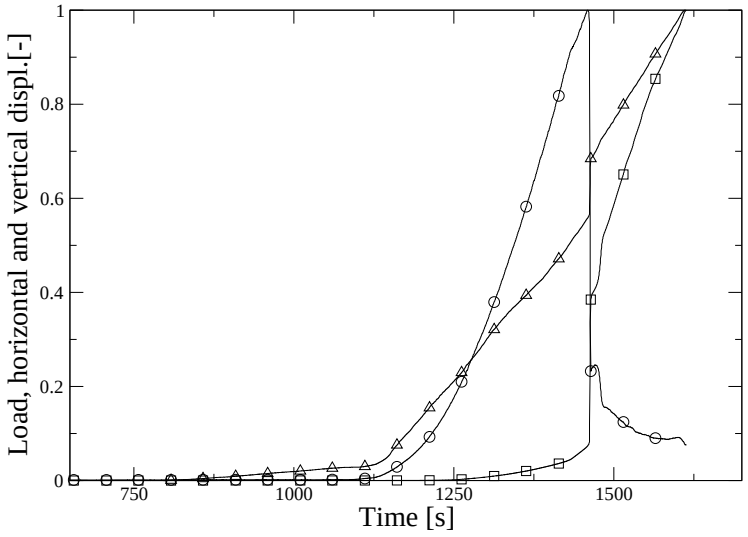

Figure 7. Experimental dimensionless results for the second specimen: (○)load, (□)horiz.displ., (△)vert.displ.

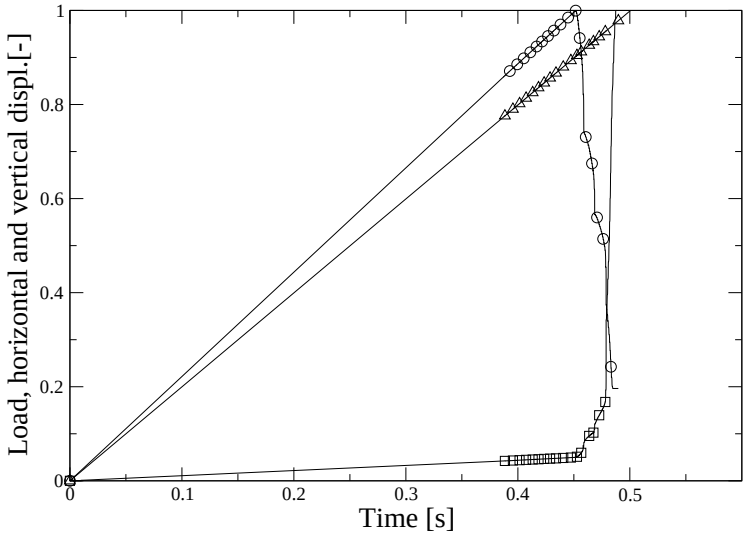

Figure 8. Numerical dimensionless results: (○)load (□) horiz.displ. (△) vert.displ.

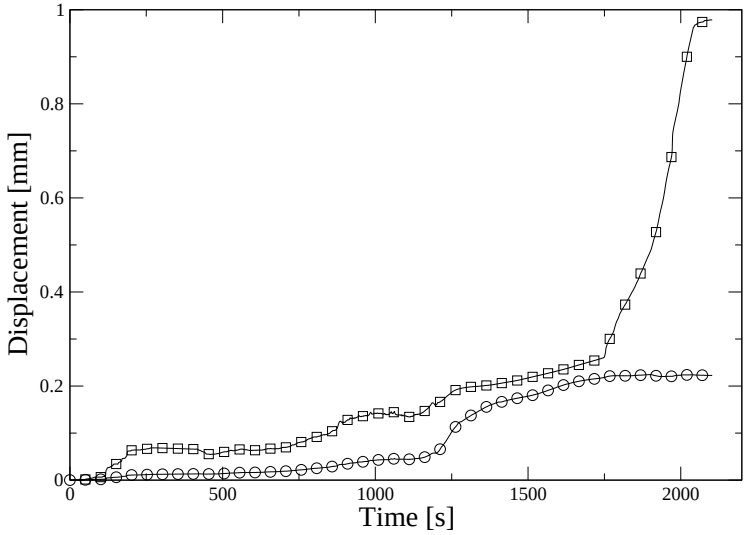

Figure 9. Experimental results for the first specimen: (○) transducer SP1, (□) transducer SP5

[4] www.3ds.com 2010 Abaqus release 6.10. *Technical report, Dassault System Simulia Corp., Providence,RI,USA*
[5] Bocca P, Carpinteri A and Valente S 1989 Fracture mechanics of brick masonry. size effects and snap-back analysis. *Materials and Structures* **22** 364-373

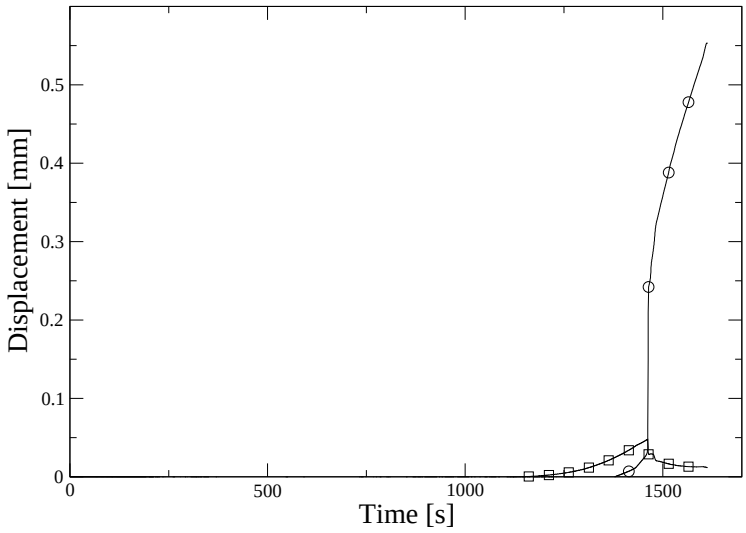

Figure 10. Experimental results for the second specimen: (○) transducer SP1, (□) transducer SP5

[6] Červenka J Kishen J M C and Saouma V E 1998 Mixed mode fracture of cementious bimaterial interfaces; part ii: Numerical simulations. *Engineering Fracture Mechanics* **60** 95-107
[7] Barpi F and Valente S 2010 The cohesive frictional crack model applied to the analysis of the dam-foundation joint *Engineering Fracture Mechanics* **77** 2182-2191
[8] Valente S 1992 Bifurcation phenomena in cohesive crack propagation. *Computers and Structures* **44** 55-62
[9] Barpi F and Valente S 1998 Size-effects induced bifurcation phenomena during multiple cohesive crack propagation. *International Journal of Solids and Structures* **35** 1851-1861

Acknowledgments

The financial support provided by the Piedmont Region through the RE-FRESCOS project is gratefully acknowledged.